NIPPON STEEL & SUMITOMO METAL TECHNICAL REPORT No. 111 MARCH 2016

Technical Report

UDC 621 . 771 . 23 . 016 . 2 : 66 . 045 . 2

Heat Transfer Technology for Steel Rolling Process

Yoshihiro SERIZAWA*
Yasuyuki TAKAMACHI
Hirohisa KAWAMURA
Hiroyuki YOSHINO
Ryuji YAMAMOTO
Shigeru OGAWA
Keiji OOGUSHI

Abstract

In steel rolling process there are many steel heating and cooling equipments. There involves many tasks concerned to heat transfer phenomena. In this article the basic research of cooling technology using water and gas jet and the research of heat conductance via solid contact area between roll and steel during rolling. The cooling technology with water and gas jet is basically studied about the heat transfer characteristic of single nozzle. The results are applied to the specification and arrangement of nozzles in the developed cooling equipments in various steel making process. The heat transfer characteristic between the roll and the steel in rolling process is studied with basic experiments and numerical simulation. The results applied to optimize the prediction of the temperature reduction in steel and the expansion of roll heated by steel in the rolling process.

1. Introduction

In the steel rolling process, steel is repeatedly heated and cooled to mold it into the desired shape and size and to impart the required qualities to it. In the hot and cold rolling processes as well as the plate manufacturing process, the heating and cooling techniques play an important role in the manufacturing of steel products according to specifications. Consider, for example, the rolls used to roll hot steel in the hot rolling process; since the rolls are subject to an increase in temperature and deformation during this process, they must be cooled in order to precisely control the shape and thickness of the steel being rolled.[1)] Thus, heat transfer techniques, including heating and cooling techniques, play a vital role in imparting the desired qualities to the steel and giving it the correct shape and size in the rolling process.

In this study on the heat transfer technique applied in steel rolling processes, we shall describe the results of our studies on the basic characteristics of water cooling with sprays, the enhancement of the performance of cooling with gas jets, and the techniques to predict heat transfer between rolls and steel in the rolling process.

2. Relationship between Spray Impact Pressure and Cooling Rate in Water Cooling

Figure 1 shows various types of nozzles that differ in their manner of spraying, and the form of spray that are used to spray water under different cooling conditions. Water spraying is a very effective cooling method as it allows the simultaneous cooling of a wide area and the flow rate of the cooling water can be easily controlled. Spray water cooling has long been studied, and heat transfer coefficients at many points of spray impingement were measured by the Iron and Steel Institute of Japan.[2)] The parameter of cooling rate around an impinging jet flow is supposed to be the local flow rate at the heat transfer surface, and the effects of the nozzle type, nozzle pressure, and so on are not completely taken into consideration. On the other hand, in the correlation for critical heat flux of an impinging jet flow system proposed by Monde et al.,[3)] the volume of water multiplied by the water flow rate is supposed to be an effective index of the impinging pressure in boiling heating. With the aim of comprehensively evaluating the various factors involved in spray cooling, which is a complex phenomenon, we studied the relationship between the impinging pressure of nozzle jet flow and heat transfer coefficient of various types of spray nozzles.

2.1 Methods of measuring impinging pressure and cooling rate

Specifications of the spray nozzles used in the experiment are shown in **Table 1**. First, to analyze the major factors in the impinging pressure of spray jet flow, we concentrated on the spray local flow rate and impinging pressure distributions. Concerning the spray

* Senior Researcher, Ph.D., Process Technology Div., Process Research Laboratories
20-1 Shintomi, Futtsu City, Chiba Pref. 293-8511

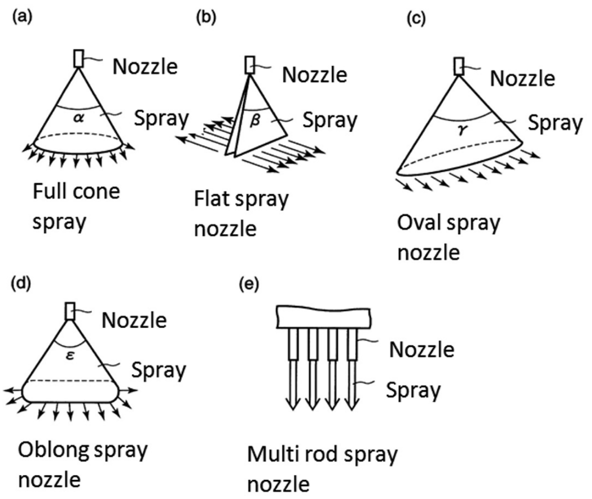

Fig. 1 Various spray nozzle

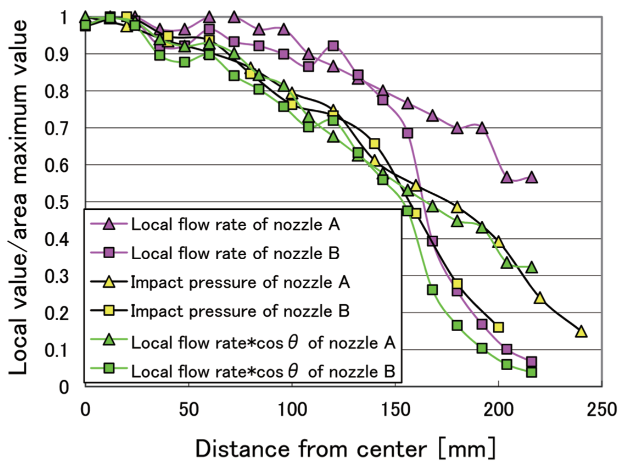

Fig. 2 Relation of impact pressure, local flow rate and (<local flow rate> * <cos θ>)

Table 1 Specifications of spray nozzle

Nozzle	Spray shape	Flow rate [L/min]	Discharge pressure [MPa]	Impact area [mm]
A	Oblong nozzle	100	0.3	250×60
B	Oval nozzle	100	0.3	300×40
C	Oval nozzle	100	0.3	350×50
D	Oblong nozzle	33	0.3	250×70
E	Full cone nozzle	100	0.3	70 ϕ

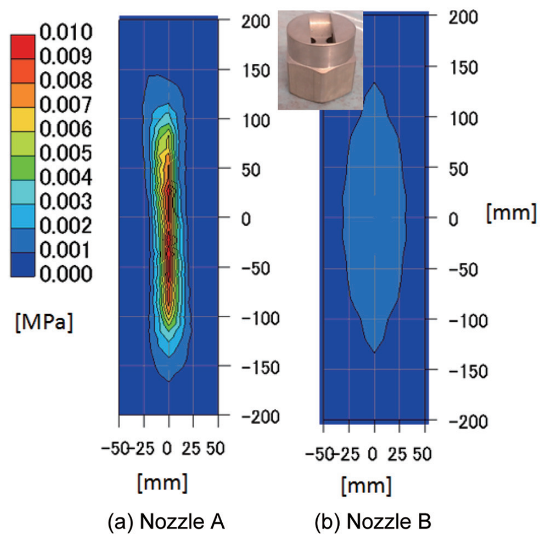

Fig. 3 Impact pressure distribution

local flow rate distribution, plastic tubes with an outside diameter of 10 mm each were arranged in parallel on the surface of impingement, and the volume of water flowing from the tubes was measured. In order to measure the impinging pressure of jet flow, water was sprayed onto a simulative steel plate and the impinging pressure was measured with a pressure sensor fitted to the steel plate. To measure the cooling rate, a 19-mm-thick SM490 (by JIS) heating test piece (heating temperature: 950°C) with a thermocouple embedded at a depth of 9.5 mm from the surface was set right above a spray nozzle and water was jetted to the test piece from below. The cooling rate at through-thickness center was obtained from the temperature history of the thermocouple embedded in the test piece.

2.2 Relationships between local flow rate, impact pressure, and cooling rate

Figure 2 shows the local flow rate, impact pressure, and impact pressure index (=the local flow rate multiplied by the cosine of spread angle of spray jet flow at the measuring point) of nozzles A and B, the values of which have been normalized as the ones right under the spray nozzle. As shown in the figure, the local flow rates and impact pressures show different tendencies. However, the values obtained by multiplying local flow rates by the cosine at the measuring point show a tendency similar to those of the impact pressures. The purpose of multiplying each local flow rate by cosine was to express the jet flow rate in the direction normal to the impinging surface at the measuring point under the assumption that the jet flow rate at the spray outlet remained the same. Consequently, the above impact pressure index represents the momentum in the direction normal to the impinging surface, which agrees well with the impact pressure for the above two types of nozzles.

The measurement results of the impact pressures of nozzles A and B are shown in **Fig. 3**. Although the two nozzles are nearly the same in terms of water flow rate and impinging area, they considerably differ in jet impact pressure. The reason could be that with nozzle A, the velocity of drops decreases during spray impingement because the spray is caused to impinge and spread near the nozzle outlet, as shown in Fig. 3.

Figure 4 shows the measurement results of cooling rate directly underneath each of nozzle. As the index of cooling rate, the average cooling rate for through-thickness center temperature range 750–600°C was used. As shown in the figure, using spray impact pressure as a parameter, it is possible to express the cooling rate of the nozzles fairly accurately, even if they differ in type and specifications. In particular, even for nozzle D that widely differs from the other nozzles in flow rate, the cooling rate is well expressed in terms of the spray impact pressure, suggesting that use of the above index is valid.

Thus, in water spray cooling, the measured impact pressure of spray from the nozzle can be used as the index of cooling rate, even for nozzles of different type and specifications or for the same noz-

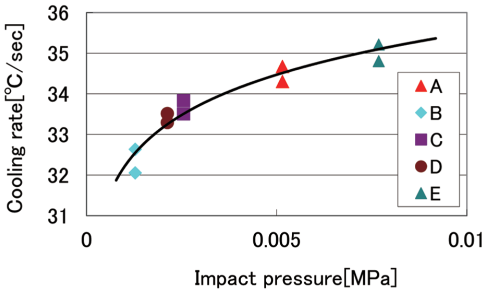

Fig. 4 Relation ship of spray impact pressure and cooling rate

zle impact area. This technique has been applied in the development of various cooling systems, such as in the primary selection of spray nozzles to be used in specific cooling equipment, the comparison between two- and one-fluid nozzles, and the modification and evaluation of nozzle internal construction.[4]

3. Enhancement of Performance of Gas Jet Cooling

Although the performance of gas jet cooling is inferior compared with that of water cooling, it is widely used in steel plate manufacturing processes because its heat transfer coefficient is unaffected by the steel plate temperature, and it permits cooling easily-oxidized hot steel plates without oxidizing them when a suitable gas is used. Enhancing the heat transfer capacity of gas jet cooling is also important for improving steel plate properties. So far, to increase jet turbulence for improving the heat transfer capacity, methods using a sound wave, installing a net inside the nozzle,[5] and utilizing a small-diameter wire[6, 7] have been reported. The last method, however, is difficult to apply on an industrial scale because the wire must be inserted into the space between the heat transfer surface and the nozzle. Therefore, it is applied only to regions where the Re number is relatively small (≤10000).

With small-diameter wires welded to the nozzle tip, we studied the effects on the heat transfer coefficient of the wire diameter, and the ratio of the distance between the nozzle and heat transfer surface to the nozzle diameter.

3.1 Experimental apparatus and procedure

The experimental apparatus and geometrical shape parameters are shown in **Fig. 5**. The nozzle cross section was circular, and the clearance between the nozzle and heat transfer surface was set to 50 mm. Nozzle diameters were 7.8, 10.5, and 12.5 mm, and wires 0.08, 0.3, 0.5, 1.0, and 1.6 mm in diameter were welded to the tip of each nozzle. The heat transfer surface was a 1-mm-thick stainless steel sheet. On the back of the heat transfer surface, K-thermocouples 0.3 mm in diameter were welded crosswise at distances of 0, 7.5, 15, 30, 45, and 60 mm from the nozzle jet impinging point. First, the heat transfer surface was electrically heated to about 600°C and then the heater was switched off and the heat transfer surface was cooled. The temperature data obtained was inputted to a computer every 0.2 s via an A/D converter board. The temperature data was used to correct the heat radiation at the back of the heat transfer surface and calculate the heat transfer coefficient. The gas flow rate was varied between 100 and 200 m/s.

3.2 Results and discussions

Figure 6 shows heat transfer coefficient distributions for heat transfer surfaces with and without a wire welded to the nozzle tip. The heat transfer coefficient distributions shown here are obtained by varying the nozzle diameter and gas flow rate. In the figure, the effect of welding a wire is clear in the vicinity of the stagnation

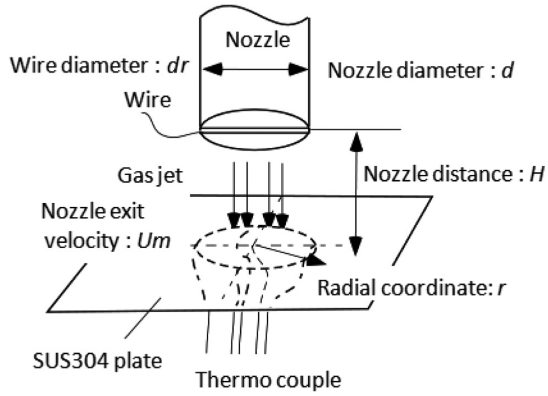

Fig. 5 Schematic diagram of experimental apparatus

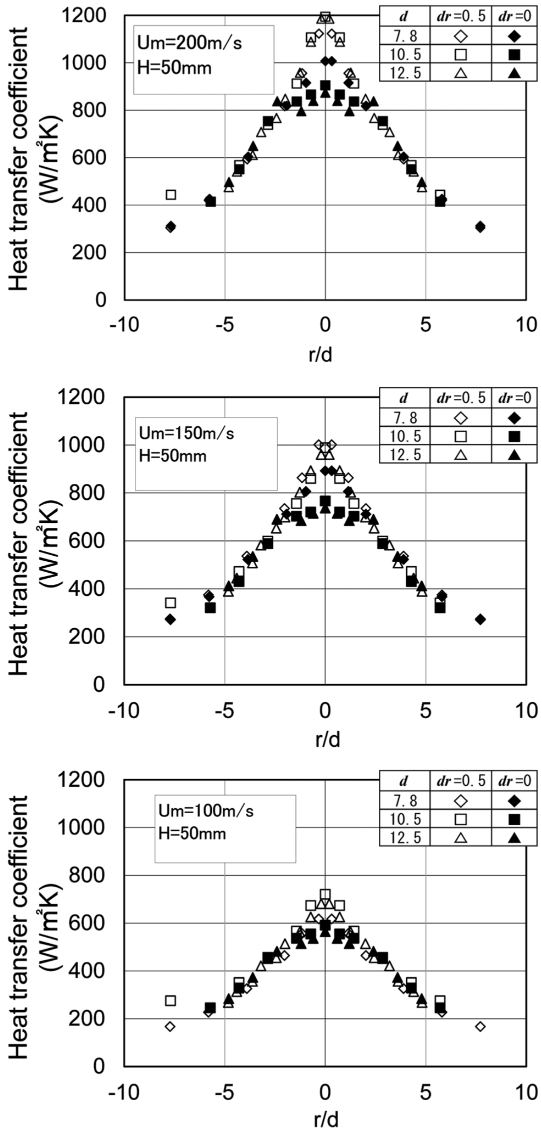

Fig. 6 Distribution of heat transfer coefficient

point $r/d<2.5$; however, when $r/d>2.5$, the effect remains almost the same regardless of the gas flow rate and the nozzle diameter. The welding a wire increased the heat transfer coefficient at and around the stagnation point, and the rate of increase in heat transfer coefficient increased as the gas flow rate was increased. This is considered to be due to an increase in turbulent flow at the center of the nozzle caused by the wire welded to the nozzle tip.

Figure 7 shows the change in heat transfer coefficient at the stagnation point when the diameter *dr* of the wire welded to the nozzle tip and the gas flow rate were varied. The nozzle diameter was 10.5 mm. The figure shows that regardless of the gas flow rate, the heat transfer coefficient at the stagnation point increases with wire diameter when $dr \leq 0.5$ mm. When $dr > 0.5$ mm, the rate of increase in heat transfer coefficient declines slightly with increasing wire diameter. However, when wires up to 1.6 mm were used in the present experiment, the rate of increase in heat transfer coefficient remained nearly the same. This suggests that in the gas flow rate range tested in this study, the effect of nozzle shape on heat transfer coefficient remains unchanged by the gas flow rate.

The effect of a change in nozzle diameter on heat transfer coefficient is shown in **Fig. 8**. Here, the gas flow rate was 150 m/s and the wire diameter was 0.5 mm. With the aim of evaluating the effect of increase in heat transfer coefficient, virtual nozzle pitches of 40 and 60 mm were set to obtain an average heat transfer coefficient within the radius equivalent to each nozzle pitch, and the effects of wire welding and nozzle diameter are demonstrated. The nozzle diameter is represented by *H*/*d*. Note that the ratio of increase in heat transfer coefficient is the ratio of heat transfer coefficient to the average heat transfer coefficient without wire welding for each nozzle diameter assumed as 1.

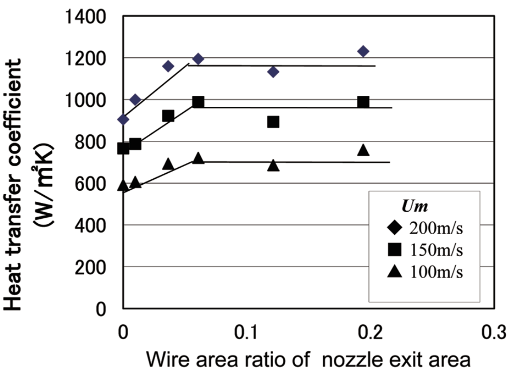

Fig. 7 Effect of wire diameter to heat transfer coefficient at the stagnation point

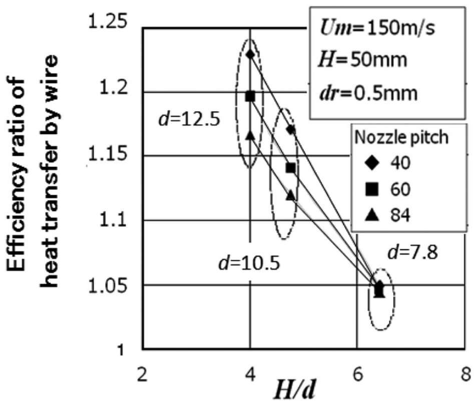

Fig. 8 Effect of nozzle pitch and *H*/*d* on heat transfer coefficient

It can be seen that as the nozzle pitch is decreased, the ratio of increase in heat transfer coefficient increases. This indicates that the average heat transfer coefficient is high when the area ratio in the neighborhood of stagnation point is high, since the increase in heat transfer coefficient by welding a wire to the nozzle is especially conspicuous around the stagnation point. Looking at the relationship between nozzle diameter and average heat transfer coefficient, the ratio of increase in average heat transfer coefficient declines as the nozzle diameter is decreased.

In Fig. 8, at the point at which the ratio of increase in average heat transfer coefficient when the nozzle diameter is made smaller than the low limit in the present experiment becomes 1, the value of *H*/*d* is in the range 7 to 8. The value indicates the point of disappearance of the so-called potential core of a gas jet.[8] The implication is that the increase in heat transfer coefficient when a wire is welded to the nozzle is due to the compensation for insufficient turbulence of the gas jet in the potential core region, and that the influence of the turbulence in the gas jet potential core region caused by a wire welded to the nozzle is small outside the potential core region. It is considered, therefore, that with the decrease in nozzle diameter, the effect of wire welding on the increase in average heat transfer coefficient decreases as the potential core area where the gas jet reaches the heat transfer surface becomes small, as shown in Fig. 8.

Figure 9 shows the evaluation results of the increase in heat transfer coefficient shown in Fig. 8. Because the welding of the wire to the nozzle causes the projected area of the nozzle port to decrease, the nozzle discharge pressure loss increases, indicating an increase in power loss. In Fig. 9, the horizontal axis represents the ratio of increase in the heat transfer coefficient when the gas flow rate was increased to the same extent as the power loss due to the welding of the wire to the nozzle. The value of the horizontal axis changes with the nozzle diameter. Specifically, the loss of pressure is determined by the ratio of wire projected area to nozzle port area, and the increase in gas flow rate corresponding to the pressure loss is determined. The increase in average heat transfer coefficient by the increase in gas flow rate corresponding to the increase in pressure loss is known for a given nozzle diameter. In Fig. 8, the effect of wire welding on the increase in heat transfer coefficient disappears when the nozzle diameter is about 6.5 mm. However, consid-

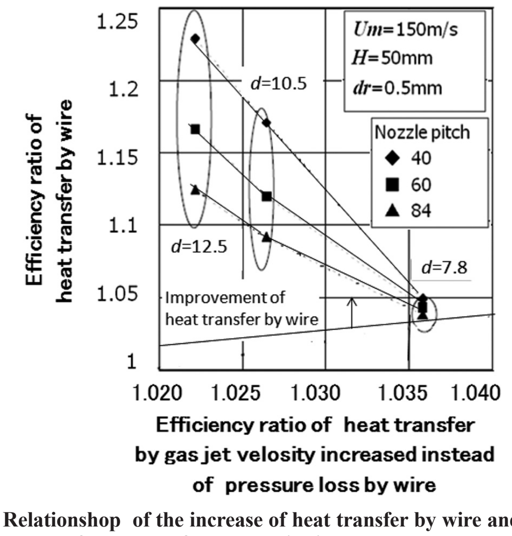

Fig. 9 Relationshop of the increase of heat transfer by wire and the increase of heat transfer by velocity increase the same as the pressure loss by wire

ering the power loss by wire welding, as shown in Fig. 9, the effect of increase in heat transfer coefficient disappears when the nozzle diameter is around 7.8 mm in the present experiment.

We studied the heat transfer characteristic of the method of welding a wire to the nozzle tip for improving the heat transfer coefficient in gas jet cooling on an industrial scale. Consequently, we found the following: 1) the increase in heat transfer coefficient by welding a wire to the nozzle is limited to the part around the stagnation point; 2) although the heat transfer coefficient improves when the projected area ratio of the wire is increased, the increase in heat transfer coefficient becomes saturated when the projected area ratio reaches a certain value; and 3) the increase in heat transfer coefficient by welding a wire to the nozzle is especially obvious when $H/d = 4–7$.

4. Heat Transfer between Solids in Contact and R&D on Technique for Predicting Heat Transfer between Steel and Rolls during Hot Rolling

Typically, in the steel manufacturing process, specifically the continuous annealing process for steel sheet, the heat transfer between solid objects in contact is utilized as a roll cooling technique, whereby a thin steel sheet under tension is made to continuously contact with the rolls.[9] On the other hand, the heat transferred from hot steel to the rolling rolls causes a thermal deformation of the rolling rolls up to several hundreds of micrometers with the time lapse.[10] However, as the thickness accuracy for hot-rolled sheet is ≤ 50 μm,[11] it is important to predict the above thermal deformation and reflect it in the thickness control operation.

So far, various studies have been conducted on heat transfer by contact. For the heat transfer by contact between stationary solid objects, Tachibana et al.[12] expressed the true contact area using the contact pressure and solid material hardness as parameters under the assumption that a gas exists in the part other than the true contact area.

Chen et al.[13] installed thermocouples on the steel side during hot rolling and obtained the contact heat transfer from the change in temperature measured by the thermocouples. They concluded that the contact pressure can be measured for low carbon, stainless, and Nb steels, and that the contact heat transfer increases as the contact pressure increases.

Hlady et al.[14] rolled aluminum and copper using the same experimental hot rolling technique used by Chen et al., suggesting that the contact heat transfer for aluminum and steel materials can be expressed by a formula when the material deformation resistance and contract pressure are taken into account. With respect to copper, however, they noted that the formula they proposed will have to be reviewed.

Yanagi et al.[15] showed that in continuous rolling of aluminum plate, the contact heat transfer between the rolls and aluminum plate can be expressed in terms of the contact arc length between the rolls and aluminum plate using the aluminum plate temperature during rolling and the roll interior temperature that becomes nearly constant after the rolling, and that the contact heat transfer increases as the contact arc length decreases.

As described above, many facts have been made known about the contact heat transfer. However, with respect to the concept of an evaluation of contact heat transfer, there is a clear need for a more detailed study.

As part of our research on the main factors in contact heat transfer aimed to develop a technique for predicting the heat transfer between steel and rolls, we studied the contact heat transfer using a short-time contact heat transfer mode wherein a moving steel sheet is pinched between rolls of various materials and clarified the characteristics of the contact heat transfer. Described below is the steel-roll heat transfer prediction technique established on the basis of the study results.

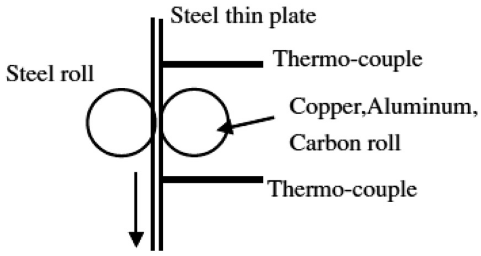

Fig. 10 Experimental apparatus of the roll contact heat transfer

Table 2 Material properties of roll

	Carbon	Alminum	Copper	Steel
Young ratio (GPa)	5	70.5	112	210
Thermal conductivity (W/m^{2}K)	93	209	394	58
Thermal diffusivity (m^2/s)	0.35	0.29	0.36	0.053

4.1 Experimental apparatus and procedure

Figure 10 shows a schematic of the experimental apparatus. Two ground rolls, each of diameter 200 mm and width 300 mm, are water-cooled internally and positioned in such a way that they pinch a moving steel sheet. A load cell is installed at each side of the rolls for measuring the pressing force applied when the steel sheet is pinched between the rolls. The steel sheet is a cold-rolled sheet 50 mm wide and 0.2–0.4 mm thick. It is continuously fed between the rolls by a feeder and a coiler installed before and after the rolls. The steel sheet is heated to about 400–500°C approximately 1 m up the roll pinching part and cooled by the rolls. The steel sheet threading speed is 15–120 m/min. The change in steel sheet temperature in the roll pinching part is measured by contact-type thermocouples at points 60 mm up and down the roll pinching part. The measurement is started after the threading of steel sheet and the condition of heating and cooling stabilize.

The thermocouples used are K-thermocouples 130 μm in diameter. They are forced to make contact with the steel sheet by a contact plate. The roll surface temperature is also measured with a thermocouple. The temperature data are inputted to a computer every 0.2 s via an A/D converter board. Using the temperature data, we corrected the temperature drop for the idle-running distance of the steel sheet except for the roll pinch section and calculated the steel sheet cooling heat and heat transfer coefficient. A steel roll was used at one side, whereas the material of the roll used at the other side was varied. The physical properties of the rolls are listed in **Table 2**. The carbon roll has a small Young's modulus and is subject to a larger deformation than the other rolls under a given contact pressure. Therefore, we estimated that with the carbon roll, the length of contact between the roll and the steel sheet becomes longer. Aluminum and copper were selected as materials having a larger thermal conductivity than iron.

4.2 Results

Figures 11 and **12** show the heat transfer coefficients of the carbon and aluminum rolls with the contact pressure and threading

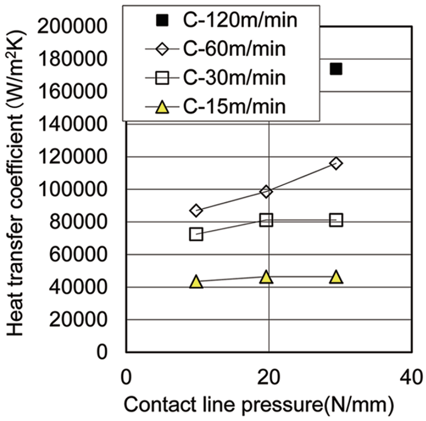

Fig. 11 Relationship of heat transfer and contact pressure with carbon roll

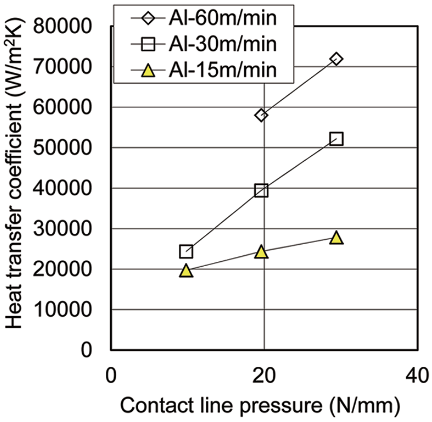

Fig. 12 Relationship of heat transfer and contact pressure with alminum roll

speed varied. The heat transfer coefficients were calculated with the length of contact between the roll and steel sheet assumed to be 1 mm. As the contact pressure, the contact line pressure was used. As shown in the figures, regardless of the roll material, the heat transfer coefficient increases as the contact line pressure and the steel sheet threading speed increase. However, the rate of increase in heat transfer coefficient differs according to the roll material and steel sheet threading speed.

For example, with the carbon roll (Fig. 11), the increase in heat transfer coefficient caused by an increase in contact line pressure remains very small when the threading speed is 15 or 30 m/min. However, when the threading speed is increased to 60 m/min, the heat transfer coefficient starts to increase monotonously. In the case of the aluminum roll (Fig. 12), the heat transfer coefficient increases monotonously under almost all threading speeds. Hence, we inferred that the contact heat transfer coefficient is proportional to the contact pressure. However, in a non-steady contact system such as these experiments, the contact heat transfer coefficient varies according to the threading speed even when the roll material and contact pressure are the same. Therefore, it is considered difficult to express the contact heat transfer by the contact pressure alone. **Figure 13** compares heat transfer coefficients among various roll materials. The carbon roll shows the highest heat transfer coefficient. As shown in the figure, the heat transfer coefficients for various roll materials differ according to the contact pressure. At a contact pressure of 30 N/mm, copper shows the second highest heat transfer coefficient, followed by aluminum and then iron. Thus, the contact heat transfer cannot be expressed by the thermal conductivity alone.

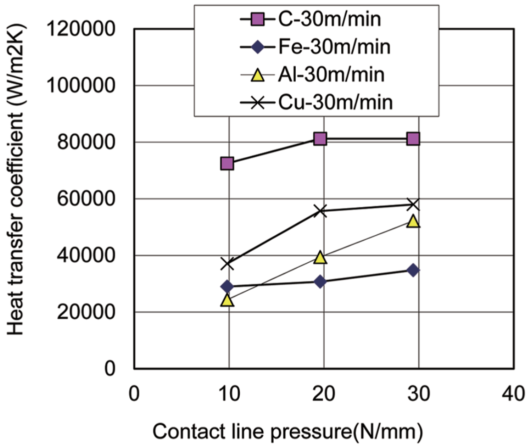

Fig. 13 Relationship of heat transfer and contact pressure with various roll material

4.3 Discussions

Thus far, we have studied the phenomenon of contact heat transfer on the basis of contact length. However, since it is difficult to express the heat transfer coefficient for each roll material, we use the concept of contact time, whereby the length of contact between the roll and steel sheet is substituted for the contact pressure. The reason is that we considered the time factor indispensable in expressing how the contact heat transfer coefficient varied according to threading speed. The method of expression is described below.

Among Herz's formulas for calculating the length of contact between solid objects,[16] the formula applicable to the contact between cylinders of different materials was used to convert the contact line pressure into the length of contact between the roll and steel sheet, while the moving speed of steel sheet was used to calculate the time of contact between the roll and steel sheet. The relationships between contact time and heat transfer coefficient obtained with carbon and aluminum rolls are shown in **Figs. 14** and **15**. It can be seen from the figures that when the difference between contact line pressure and steel sheet threading speed is expressed in terms of contact time, contact heat transfer coefficient shows a good correlation with contact time. The reason the heat transfer coefficient at the time of contact between solid objects can be expressed by the contact time, as shown in Figs. 14 and 15, is considered as follows.

When the contact time is short, the heat transfer from the steel sheet to roll takes place without being affected by the heat transfer on the roll side; hence, a high heat transfer coefficient can be obtained. However, as the contact time increases, the heat transferred to the roll side partly resides in the roll temporarily, causing the roll surface temperature to increase. As a result, the heat transfer declines, and the heat transfer coefficient decreases. This is considered to be a phenomenon which is governed by heat conductivity, similar to the one in which the maximum cooling rate at the through-thickness center of the steel sheet declines as the steel sheet is increased in thickness.

However, it follows that even if the threading speed and contact line pressure can be expressed by the contact time for a specific roll material, we see only the difference made by the Young's modulus of the roll when rolls of different material are involved. Therefore,

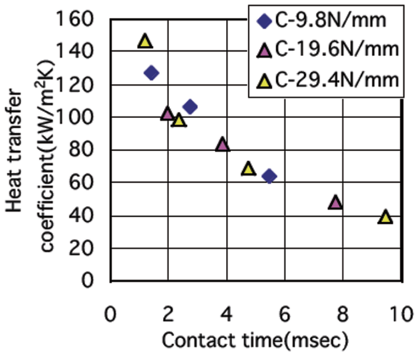

Fig. 14 Relationship of heat transfer and contact time with carbon roll

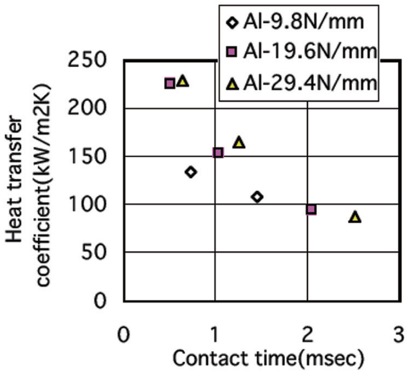

Fig. 15 Relationship of heat transfer and contact time with alminum roll

in **Fig. 16**, the relationships between contact time and heat transfer coefficient for various roll materials are shown. According to the figure, the heat transfer coefficient of copper is large when the contact time is about 2 ms. This is probably due to the fact that the effects of the thermal properties of the roll materials are not considered.

So, to give due consideration to the thermal properties of the roll materials, we formulated the heat balance inside the roll within the contact time as follows.

$$q = h\left(Ts - Tr\right) = \lambda\left(Ts - Tr\right) / Lt \quad (1)$$

$$Lt = A\sqrt{(\kappa t)} \quad (2)$$

where q: heat flux (W/m^2), h: roll-steel heat transfer coefficient (W/m^{2}K), Ts: steel temperature (K), Tr: roll temperature (K), λ: roll material thermal conductivity (W/mK), Lt: thermal diffusion depth in contact time (m), A: coefficient, κ: roll material thermal diffusivity (m^2/s) = λ/ρc, ρ: density (kg/m^3), c: specific heat (J/kg/K), and t: roll-steel contact time (s). Using the thermal property index [$\lambda/\sqrt{(\kappa t)}$] derived from the above equations, relationships between thermal properties of various roll materials and the heat transfer coefficient, h, are shown in **Fig. 17**.

The above index is the heat conductivity of roll material divided by the index of thermal diffusion depth within contact time, as shown in **Fig. 18**. It indicates the average heat flux in the roll within the contact time and has the same dimension as the heat transfer coefficient. According to Fig. 17, when the thermal conductivity relative to the thermal diffusion depth within the contact time is high, the heat transfer coefficient becomes high. Thus, we consider that the heat transfer between the roll and steel sheet can be expressed in terms of the contact time and the thermal properties of the roll and steel sheet.

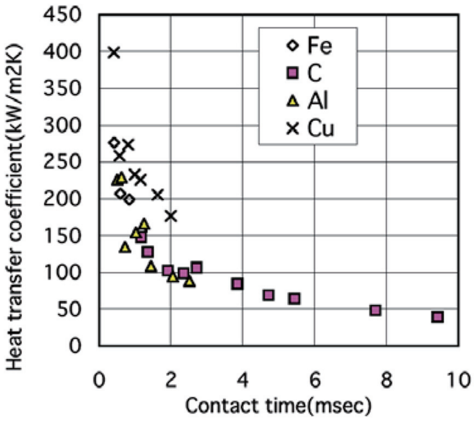

Fig. 16 Relationship of heat transfer and contact time with various roll material

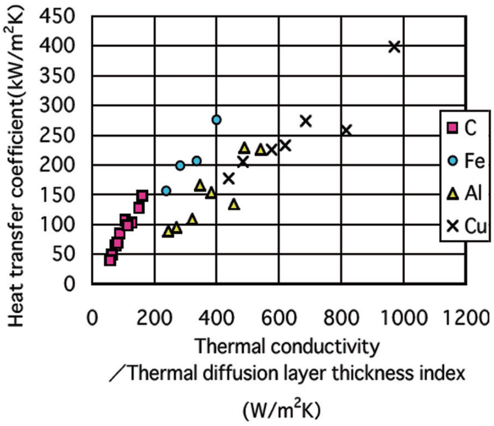

Fig. 17 Relationship of heat transfer and 'thermal conductivity by thermal diffused depth' of various roll material

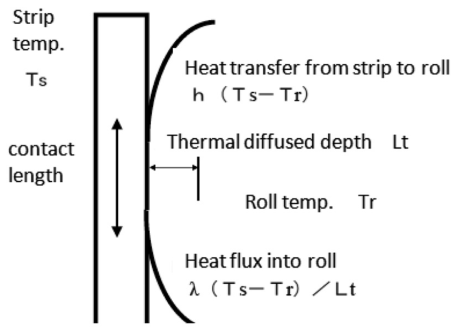

Fig. 18 Heat transfer appratus between roll and strip

4.4 Development of steel-roll heat transfer model

On the basis of the results described in Section 4.3, we considered that when the heat transfer between solid objects occurs as their surfaces are crushed, as in rolling, it would be possible to calculate the heat transfer coefficient by taking into account the material thermal properties and contact time. Therefore, we created a calculation model. As shown in **Fig. 19**, for the purpose of the calculations, we adopted a one-dimensional, non-steady heat transfer equation,[17] with the heat transfer in the roll circumferential direction and steel

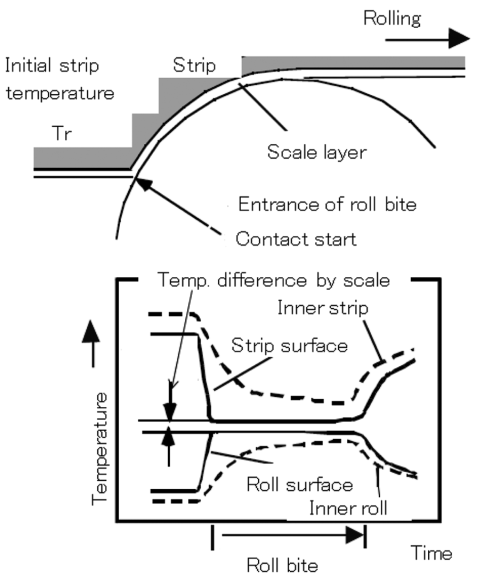

Fig. 19 Temperature trasition in roll and strip

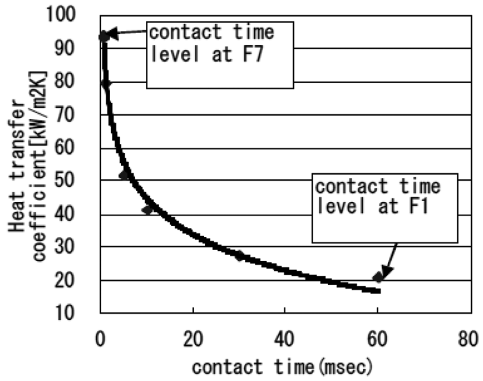

Fig. 20 Effect of the contact time on heat transfer between roll and strip

rolling direction left out of consideration. We assumed that after the start of contact, the rolling roll and steel form a single unit with a film of iron oxide sandwiched between them. In addition, we considered the frictional heat during rolling, and the heat generated during deformation of the steel being rolled.[18] The heat transfer from the start to the end of contact between the roll and steel was calculated, and the change in heat transferred to the roll during that time converted in terms of contact time and contact length was assumed to be the average heat transfer coefficient during the contact between the roll and steel.

Next, as the factors influencing the heat transfer coefficient to be determined by the developed model, the influences of contact time and roll temperature before the start of contact were calculated. The calculation results are shown in **Figs. 20** and **21**. As shown in Fig. 20, the influence of roll-steel contact time is very strong, as reported by Yanagi et al. From Fig. 21, it can be seen that the influence of the initial roll temperature is negligibly small, even when it changes from 50 to 200°C.

Figure 21 shows the heat transfer coefficients calculated with the developed model using actual rolling operation data. **Figure 22** shows the heat transfer coefficients calculated for seven finish rolling stands when the strip thickness was varied after finish rolling.

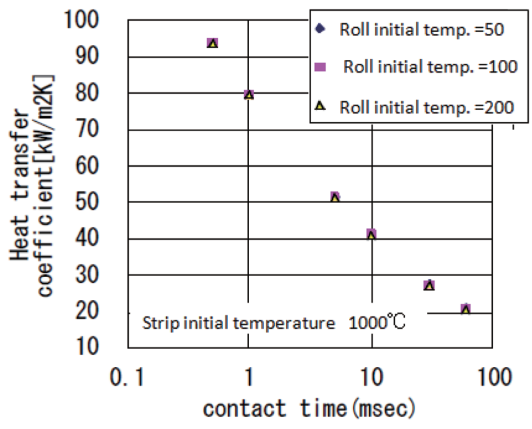

Fig. 21 Effect of roll temperature on heat transfer

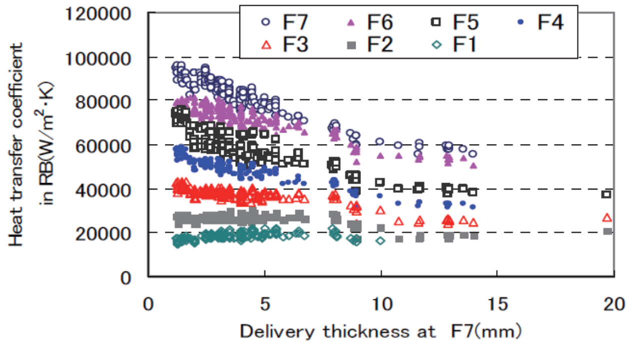

Fig. 22 Calculating heat transfer coefficient in roll bite

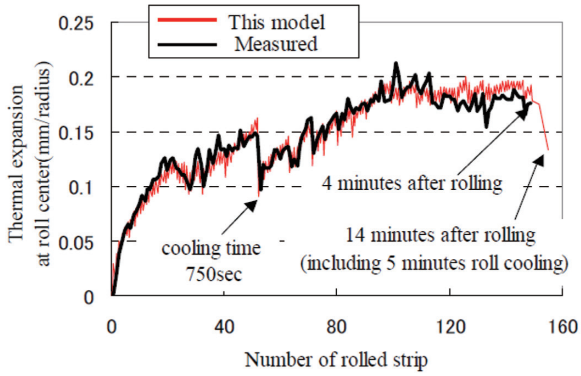

Fig. 23 Comparison of thermal expansion

F7 means the 7th stand of finishing rolling machine, and F1, F2, F3, F4, F5, F6 are the same meaning with F7. It can be seen from the figure that the heat transfer coefficient, including the heat transfer ratio between the stands, changes in a complicated manner according to the strip thickness after the finish rolling.

Figure 23 shows the results of a comparison between measured and calculated thermal expansions of rolling rolls. They agree well, proving that the developed model enables one to accurately predict the thermal expansion behavior of actual rolling rolls.

5. Conclusion

We have described examples of our Research & Development on the heat transfer technique in steel rolling processes, specifically the results of fundamental studies on water cooling/gas jet cooling and the development of a model for predicting the heat transfer between rolling rolls and steel. In recent years, with the ever-increasing demand for steel products of higher strength and higher dimensional accuracy, and the need to deliver this while reducing CO_2 emissions, problems relating not only to the heating and cooling technique, but also the heat transfer technique in steel rolling processes have become increasingly complicated. We intend to continue tackling these problems by developing new heat transfer techniques to reduce the load of steel manufacturing processes by taking into consideration basic factors in heat transfer phenomena.

References

1) The Iron and Steel Institute of Japan: Ita atsuen no riron to jissai. 2010, p. 151
2) The Iron and Steel Institute of Japan: Kouzai No kyousei reikyaku. Special Report No. 29, 1978, p. 4
3) Monde, M.: Transactions of the JSME. 50-453B, 1392 (1984)
4) International Unexamined Patent: WO2014/102909 A1. 2014.7.3
5) Gardon, R., Akifirat, J.C.: Int. J. Heat Trans. 8, 1261 (1965)
6) Hada, Y. et al.: 33rd National Heat Transfer Symposium of Japan. 1996, p. 617
7) Hada, Y. et al.: Transactions of the JSME. 66-644B, 1176 (2000)
8) The Japan Society of Mechanical Engineers: Heat Transfer Engineering Data. 5th Edition. 2009, p. 37
9) Japanese Unexamined Patent: Unexamined Patent Application 11-236622. 1999. 8. 31
10) The Iron and Steel Institute of Japan: Ita atsuen no riron to jissai. 2010, p. 155
11) Nippon Steel Corporation: Tetsu to tekkou ga wakaru hon. 2004, p. 96
12) Tachibana: Journal of the Japan Society of Mechanical Engineers. 155, 102 (1952)
13) Chen, W.C. et al.: Metal. Trans. A. 24A, 1307 (1993)
14) Hlady, C.O. et al.: Metal. Mat. Trans. B. 26B, 1019 (1995)
15) Yanagi, S., Ikeda, M., Kunii, H.: Kobe Steel Technical Report. 58 (3), 29 (2008)
16) Murakami, T.: Dansei kougaku. 1996, p. 166
17) Mizutani, Y., Kouzuki, M.: Computer ni yoru netsu-idou to nagare no suuti-kaiseki. 1985, p. 56
18) Shida, S.: Journal of JSTP. 9, 127 (1968), 10, 610 (1969)


Yoshihiro SERIZAWA
Senior Researcher, Ph.D.
Process Technology Div.
Process Research Laboratories
20-1 Shintomi, Futtsu City, Chiba Pref. 293-8511


Ryuji YAMAMOTO
Senior Manager
Plate Div.
Kimitsu Works


Yasuyuki TAKAMACHI
Chief Researcher
Steel Rolling Research Lab.
Process Research Laboratories


Shigeru OGAWA
Executive Advisor, Dr.Eng.


Hirohisa KAWAMURA
Senior Manager, Head of Dept.
Cold Rolling & Processing Plant Engineering Dept.
Plant Engineering Div.
Plant Engineering and Facility Management Center


Keiji OOGUSHI
Senior Manager
Processing Line Engineering Gr., Engineering & Development Section, Steel Plant Engineering Dept.-II,
Plant & Machinery Division
Nippon Steel & Sumikin Engineering Co., Ltd.


Hiroyuki YOSHINO
Senior Researcher
Process Technology Div.
Process Research Laboratories